Available online at www.sciencedirect.com
SCIENCE DIRECT
Trans. Nonferrous Met. Soc. China 16(2006) 800−807
Transactions of Nonferrous Metals Society of China
www.csu.edu.cn/ysxb/

Effects of rapid quenching on microstructures and electrochemical properties of $La_{0.7}Mg_{0.3}Ni_{2.55}Co_{0.45}B_x$($x$=0−0.2) hydrogen storage alloy

ZHANG Yang-huan(张羊换)[1,2], DONG Xiao-ping(董小平)[1], WANG Guo-qing(王国清)[2],
GUO Shi-hai(郭世海)[2], REN Jiang-yuan(任江远)[1], WANG Xin-lin(王新林)[2]

1.School of Material, Inner Mongolia University of Science and Technology, Baotou 014010, China;
2.Department of Functional Material Research, Central Iron and Steel Research Institute, Beijing 100081, China

Received 29 August 2005; accepted 1 April 2006

Abstract: In order to improve the electrochemical performances of La-Mg-Ni based electrode alloys with $PuNi_3$-type structure, a trace of boron was added in $La_{0.7}Mg_{0.3}Ni_{2.55}Co_{0.45}$ alloy. The $La_{0.7}Mg_{0.3}Ni_{2.55}Co_{0.45}B_x$($x$=0, 0.05, 0.1, 0.15 and 0.2) alloys were prepared by casting and rapid quenching. The electrochemical performances and microstructures of the as-cast and quenched alloys were investigated. The effects of rapid quenching on the microstructures and electrochemical performances of the above alloys were investigated. The results show that the as-cast and quenched alloys are composed of (La, Mg)Ni_3 phase, $LaNi_5$ phase and $LaNi_2$ phase. A trace of the Ni_2B phase exists in the as-cast alloys containing boron, and the Ni_2B phase in the B-contained alloys nearly disappears after rapid quenching. Rapid quenching increases the amount of the $LaNi_2$ phase in the B-free alloy, but it decreases the amount of the $LaNi_2$ phase in the boron-containing alloys. The effects of rapid quenching on the capacities of the boron-containing and boron-free alloys are different. The capacity of the B-free alloy monotonously decreases with increasing quenching rate, whereas the capacities of the B-contained alloys have a maximum value with the change of the quenching rate. The rapid quenching can improve the stability of La-Mg-Ni based electrode alloy but lowers the discharge plateau voltage and decreases the plateau length. The effect of rapid quenching on the activation capabilities of the alloys was complicated.

Key words: La-Mg-Ni based electrode alloys; rapid quenching; microstructures; electrochemical properties

1 Introduction

Ni-MH batteries have been used widely by virtue of several of their advantages, such as high capacity, capable of performing a high rate charge/discharge, high resistance to overcharging and over-discharging, a long cycle life, environmental friendliness, and inter-changeability with Ni-Cd batteries[1]. Since the commercialization of small size Ni-MH cells in 1990, the small size Ni-MH cells have rapidly grown and gained a good share in the rechargeable battery market. In the very recent years, however, the rechargeable Ni-MH cells are encountering serious competition from Li-ion cells since the Li-ion cells show higher energy density than the Ni-MH cells per unit mass or volume. On the other hand, the production cost of Ni-MH battery based on the current hydride technology also limits the widespread applications as power sources of electric vehicles or hybrid cars because low-cost Pb-acid batteries are still dominating over the segment. Therefore, investigations of new type electrode alloys with higher capacity and longer cycle life is extremely important to exalt the competition ability of Ni-MH batteries in the rechargeable battery field. A series of metal hydride electrode materials have been discovered, including the rare-earth-based AB_5-type alloys[2], the Laves phase AB_2-type alloys[3], the V-based solid solution alloys[4], and the Mg-based alloys[5]. Among the hydrogen storage alloys mentioned above, the discharge capacity of the AB_5-type electrode alloys is comparatively low, the activation of the AB_2-type Laves phase electrode alloys is very difficult, the electrocatalytic activation of the V-based solid solution alloys is also difficult, and the cycle stability of the Mg-based electrode alloy is extremely poor. Especially, the electrochemical capacity

Foundation item: Project(50131040) supported by the National Natural Science Foundation of China; Project(20050205) supported by the Key Technology Research and Development Program of Inner Mongolia Province, China; Project(NJ05064) supported by the Higher Education Science Research Project of Inner Mongolia Province, China
Corresponding author: ZHANG Yang-huan; Tel: +86-10-62187570; E-mail: zyh59@yahoo.com.cn, zhangyh59@163.com

of currently advanced AB_5-type materials has reached 320−340 mA·h/g at 0.2−0.3*C* rate and room temperature. It seems to be difficult to further improve the capacity of the AB_5-type alloy since the theoretical capacity of $LaNi_5$ is about 372 mA·h/g. Several new and good hydrogen storage alloys were reported recently. One of the most promising candidates is the La-Mg-Ni based alloy for increasing the capacity. KADIR et al[6] investigated the structure of the R_2MgNi_9 (R=La, Ce, Pr, Nd, Sm and Gd) alloys and the result obtained shows that the alloys have the $PuNi_3$-type structure. After investigating the electrochemical performances of the La_2MgNi_9, $La_5Mg_2Ni_{23}$ and La_3MgNi_{14}-type electrode alloys, KOHNO et al[7] found that the $La_5Mg_2Ni_{23}$-type electrode alloy $La_{0.7}Mg_{0.3}Ni_{2.8}Co_{0.5}$ has a capacity of 410 mA·h/g and good cycle stability during 30 charge-discharge cycles. PAN et al[8] investigated the structures and electrochemical characteristics of the $La_{0.7}Mg_{0.3}(Ni_{0.85}Co_{0.15})_x$ (x=3.15−3.80) alloy system and obtained a maximum discharge capacity of 398.4 mA·h/g, but the cycle stability of the alloy needs to be improved further. In order to further improve the cycle stability of the La-Mg-Ni based $La_{0.7}Mg_{0.3}Ni_{2.55}Co_{0.45}$ electrode alloy, a trace of boron was added and rapid quenching technique was used in the preparation of the alloys. The obtained results indicated that the addition of boron and the rapid quenching could enhance the cycle lives of the alloys.

2 Experimental

2.1 Preparation of alloys

The chemical composition of the investigated alloys is $La_{0.7}Mg_{0.3}Ni_{2.55}Co_{0.45}B_x$ (x=0, 0.05, 0.10, 0.15 and 0.20). These alloys are represented by M_0, M_1, M_2, M_3 and M_4, respectively. The purity of all the component metals (La, Ni, Co, Mg) is at least 99.8%. The purity of boron is 99.93%. The experimental alloys were melted in an argon atmosphere using a vacuum induction furnace. A binary La-Mg intermediate alloy (30%Mg+70%La) was beforehand prepared by electrolytic synthesis and a positive argon pressure of 0.1 MPa was applied for preventing the volatilization of magnesium during melting. After induction melting, the melt was poured into a copper mould cooled by water, and a cast ingot was obtained. Part of the as-cast alloys was re-melted and quenched by melt-spinning with a rotating copper wheel. Flakes of the as-quenched alloys were obtained with quenching rates of 15, 20, 25 and 30 m/s. The quenching rate is expressed by the linear velocity of the copper wheel.

2.2 Microstructure determination and morphology observation

The polished samples were etched with a 60% HF solution. The morphologies of the as-cast and quenched alloys were examined by SEM. The microscopic composition of the as-cast alloys was analysed by EDX. The phase structures and compositions of the alloys were determined by XRD diffractometer of D/max/2400. The diffraction was performed with $CuK_{\alpha 1}$ radiation filtered by graphite. The powder samples were dispersed in anhydrous alcohol for observing the grain morphology with TEM, and for determining crystalline state of the samples with selected area electron diffraction(SAD). The granular morphologies of the alloy electrode before and after electrochemical cycling were observed by SEM in order to reveal the mechanism of the efficiency loss of the alloy electrode.

2.3 Electrode preparation and electrochemical measurement

A round electrode pellets with 15 mm diameter were prepared by mixing 1 g alloy powder and 1 g Ni powder as well as a small amount of polyvinyl alcohol (PVA) solution as binder, and then compressing under a pressure of 35 MPa. After drying for 4 h, the electrode pellets were immersed in 6 mol/L KOH solution for 24 h in order to wet the electrodes fully before the electrochemical measurement.

The experimental electrodes were tested in a tri-electrode open cell, consisting of a working electrode (metal hydride electrode), a counter electrode ($NiOOH/Ni(OH)_2$) and a reference electrode (Hg/HgO). In order to reduce the ohmic drop between the working electrode and the reference electrode, a Luggin capillary was located close to the hydride electrode in the working electrode apartment. The electrolyte was a 6 mol/L KOH solution. The voltage between the negative electrode and the reference electrode is defined as the discharge voltage. Every cycle was charged with constant current of 100 mA/g for 5 h, resting 15 min and then discharged at 100 mA/g to −0.500 V cut-off voltage. The environment temperature of measurement was kept at 30 ℃.

3 Results and discussion

3.1 Effects of rapid quenching on microstructures

3.1.1 Phase composition and structure

The XRD patterns of the as-cast and quenched alloys are shown in Fig.1. It can be seen from Fig.1 that the alloys have a multiphase structure, composing of (La, Mg)Ni_3 phase and $LaNi_5$ phase as well as $LaNi_2$ phase. A trace of Ni_2B phase exists in the as-cast boron-contained alloy, and the abundance of Ni_2B phase increases with increasing the boron content. The addition of boron and the rapid quenching have an obvious influence on the phase composition of the alloys. It can also be seen from

Fig.1(a) that the relative amount of $LaNi_2$ phase in the as-cast alloy significantly increases with increasing boron content. Probably, the formation of Ni_2B phase also implies the formation of $LaNi_2$ phase. It can be derived by comparing the diffraction peaks of the $LaNi_2$ phase in the as-cast and quenched M_0 alloys that rapid quenching can increase the amount of $LaNi_2$ phase in the M_0 alloy, but it leads to a decreased amount of $LaNi_2$ phase in the B-contained alloys. Obviously, it is ascribed to a distinct decrease of Ni_2B phase in the B-containing alloy after rapid quenching.

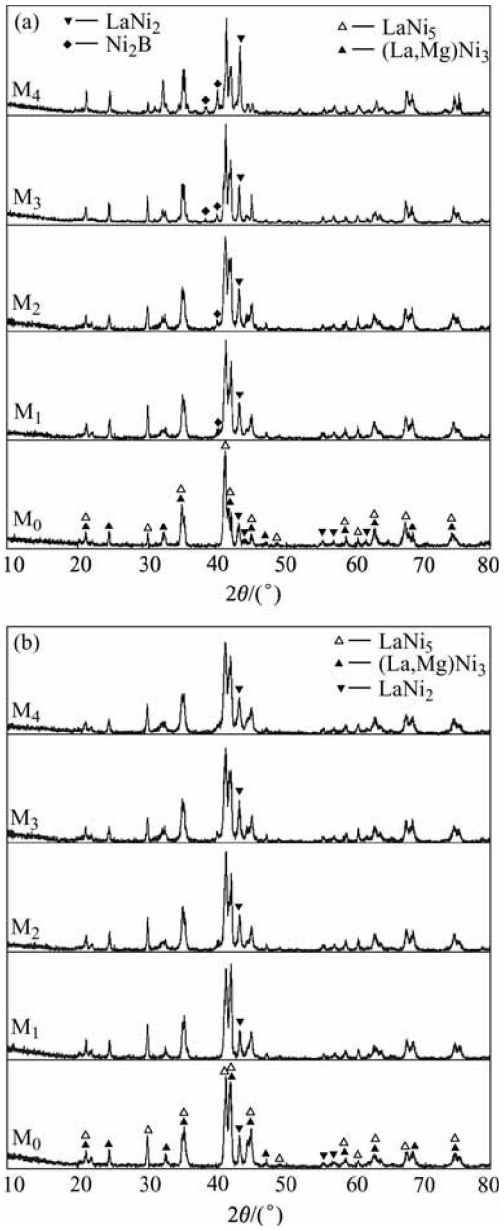

Fig.1 XRD patterns of as-cast and quenched alloys: (a) As-cast; (b) As-quenched (20 m/s)

3.1.2 Microstructure and morphology

The morphologies of the as-cast and quenched alloys were inspected by SEM, and the results are shown in Fig.2. The results obtained by EDX indicated that all the experimental alloys are of multiphase structure, containing both (La, Mg)Ni_3 phase (white grey regions) and $LaNi_5$ phase (black grey regions). Because the amount of $LaNi_2$ phase is small and it affects (La, Mg)Ni_3 phase in the process of growing, it is difficult to see the morphology of $LaNi_2$ phase. A morphology of (La, Mg)Ni_3+$LaNi_2$ structure with a eutectic character can be seen clearly in the as-cast M_4 alloy by virtue of Ni_2B phase promoting the formation of $LaNi_2$ phase. The amount of Ni_2B is too small to be distinguished. It can be seen from Fig.2 that the grains of the as-cast alloys are very coarse and the composition homogeneity is very poor. Compared with the morphologies of the as-cast alloys, the rapid quenching markedly refined the grains and significantly improved the composition homogeneity of the alloys. The morphologies and the crystalline state of the as-quenched alloys were examined by TEM, and the results are shown in Fig.3. The results obtained by SAD show that the as-quenched M_0 and M_2 alloys have a multiphase structure and an obvious tendency to amorphous phase formation in the M_2 alloy, and some amount of amorphous phase existed in the M_4 alloy. It can be seen from Fig.3 that the morphology of the as-quenched M_0 alloy presents a typical microcrystalline character, and an amorphous and nanocrystalline phase co-exist in the as-quenched M_2 alloy. It indicates that the formation abilities of an amorphous phase in the alloys are different although the same rapid quenching technique was used. Obviously, it can be attributed to the action of boron. The relative mechanism of boron addition promoting the formation of an amorphous phase has been reported in Ref.[9].

3.2 Effects of rapid quenching on electrochemical performances

3.2.1 Discharge capacity

The maximum discharge capacities of the as-cast and quenched alloys were measured with a constant current density of 100 mA/g, and the quenching rate dependence of the maximum discharge capacity of the alloys was illustrated in Fig.4. Fig.4 shows that the effects of the quenching rate on the capacities of the B-containing and B-free alloys are different. The capacity of the M_0 alloy monotonously decreases with the increase of the quenching rate, whereas the capacities of all alloys except M_0 alloy have a maximum value with the change of the quenching rate. Obviously, it is directly relevant to the structure change of the alloys resulted from rapid quenching. For the B-free alloy, rapid quenching increases the amount of $LaNi_2$ phase (Fig.1). The lattice internal stress increases with increasing the quenching rate, which is unfavourable for the capacity of

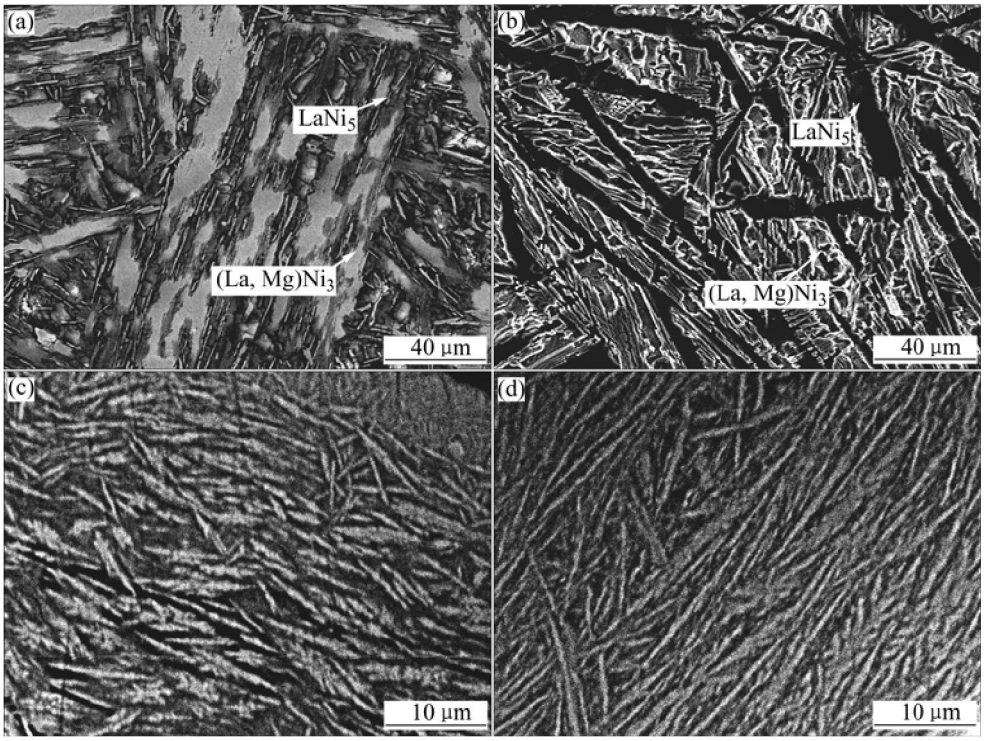

Fig.2 SEM morphologies of as-cast and quenched alloys: (a) As-cast M_1 alloy; (b) As-cast M_4 alloy; (c) As-quenched M_1 alloy; (d) As-quenched M_4 alloy

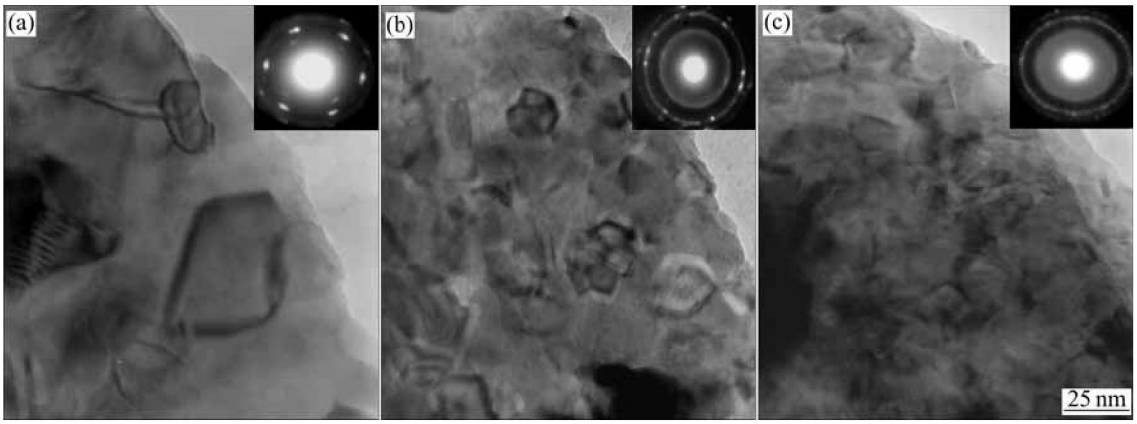

Fig.3 TEM morphologies of SAD patterns of as-quenched (20 m/s) alloys: (a) M_0; (b) M_2; (c) M_4

the alloy. Because the capability of the hydrogen absorption of $LaNi_2$ phase is much lower than that of (La, Mg) Ni_3 phase and $LaNi_5$ phase, it seems to go without saying that the capacity of the alloys decreases monotonously with increasing the quenching rate. For the B-containing alloys, the rapid quenching leads to approximate disappearance of Ni_2B phase, which hampers the formation of $LaNi_2$ phase. The decrease of the amounts of Ni_2B phase and $LaNi_2$ phase is favourable for the increase of the discharge capacity of the alloy. Therefore, the discharge capacities of the alloys increase with increasing the quenching rate. On the other hand, Boron addition promotes the formation of an amorphous phase in the alloy, which is unfavourable for the increase of the discharge capacity of the alloy because the capacity of the amorphous phase is half as large as that of the crystalline alloy[10]. Therefore, the higher the quenching rate, the larger the amount of amorphous phase and the lower the discharge capacity.

3.2.2 Activation capability

The activation number denoted by n was characterized by the number of charge-discharge cycles required for attaining the greatest discharge capacity through a charge-discharge cycle at a constant current density. The cycle number dependence of the discharge capacities of the as-cast and quenched alloys was

illustrated in Fig.5, the charge-discharge current density being 100 mA/g. It can be derived from Fig.5 that all of the as-cast and quenched alloys have an excellent activation performance, and the as-cast and quenched alloys could be activated completely after 2 to 4 cycles. The effect of rapid quenching on the activation capability of the alloys is complicated. Generally, the activation capability of the hydrogen storage alloy is directly related to the change of the internal energy of the system before and after absorbing hydrogen. The larger the additive internal energy, which originates from the oxidation film formed on the surface of the electrode alloy, and the strain energy, which is produced by hydrogen atom entering the interstitial of the tetrahedron or octahedron of the alloy lattice, the poorer the activation performance of the alloy[11]. Obviously, some parameters, such as the phase structure, the surface characteristics, the grain size and the interstitial dimensions of the alloy, are decisive factors of the activation performance of the alloy. The fact that the as-cast and quenched alloys have good activation performance is mainly ascribed to their multiphase structures because the phase boundary can decrease the lattice distortion and strain energy formed in the process of hydrogen absorption. Moreover, the phase boundary provides good tunnels for diffusion of hydrogen atoms, the activation capability of the alloys being improved significantly[12].

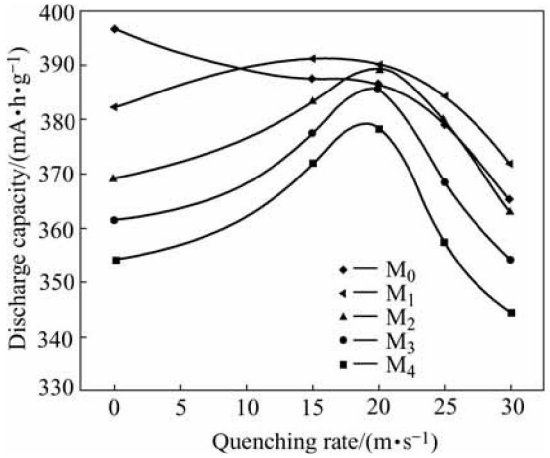

Fig.4 Quenching rate dependence on discharge capacity of alloys

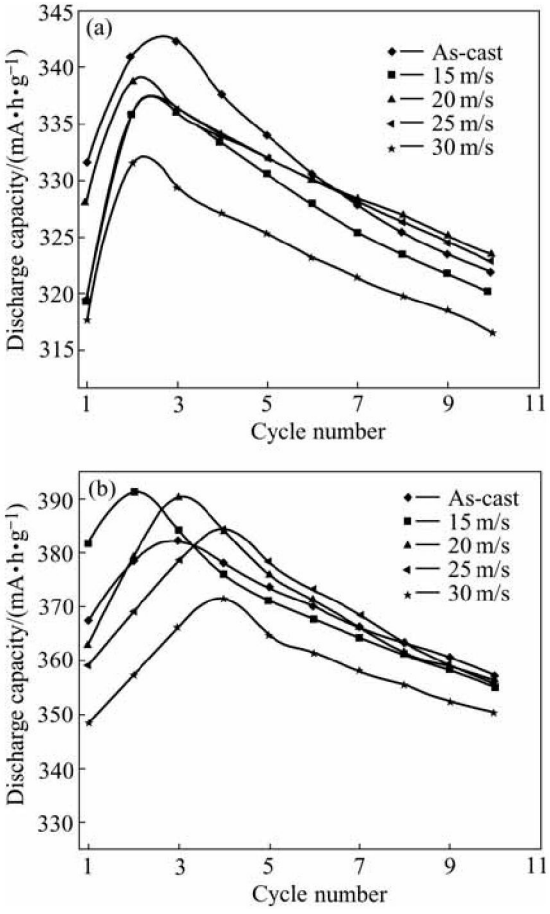

Fig.5 Activation performances as-cast and quenched alloys at different quenching rates: (a) M_0; (b) M_1

3.2.3 Discharge voltage characteristic

The discharge voltage characteristic is an important performance of the electrode alloy, which was characterized by the voltage plateau of the discharge voltage curve of the alloy. The longer and the more horizontal the discharge voltage plateau, the better the discharge characteristics of the alloys. In order to compare the characteristics of the discharge voltage plateau, the discharge voltage curves of the alloys with different quenching rates are shown in Fig.6. It can be derived from Fig.6 that rapid quenching lowers the discharge plateau voltage and decreases the plateau length. When quenching rate is larger than 20 m/s, the slopes of the discharge voltage plateaus of the alloys obviously increase with the increase of the quenching rate.

3.2.4 Cycle life

The cycle life, indicated by N, is characterized by the cycle number after which the discharge capacity of the alloy obtained with a current density of 100 mA/g is reduced to 60% of the maximum capacity. The cycle number dependence of the discharge capacities of the as-cast and quenched alloys is shown in Fig.7. It can be derived from Fig.7 that the slopes of the curves of the alloys decrease with the increase of the quenching rate. This indicates that the rapid quenching is favourable for the improvement of the cycle stabilities of the alloys. In order to show the effect of the quenching rate on the cycle lives of the alloys, the quenching rate dependence of the cycle lives of the alloys is presented in Fig.8. Fig.8 shows that the cycle lives of the alloys increase with the increase of the quenching rate. When the quenching rate increases from 0 (As-cast was defined as quenching rate of 0 m/s) to 30 m/s, the cycle lives of M_0 and M_2 alloys

increase from 72 and 86 cycles to 100 and 106 cycles, respectively.

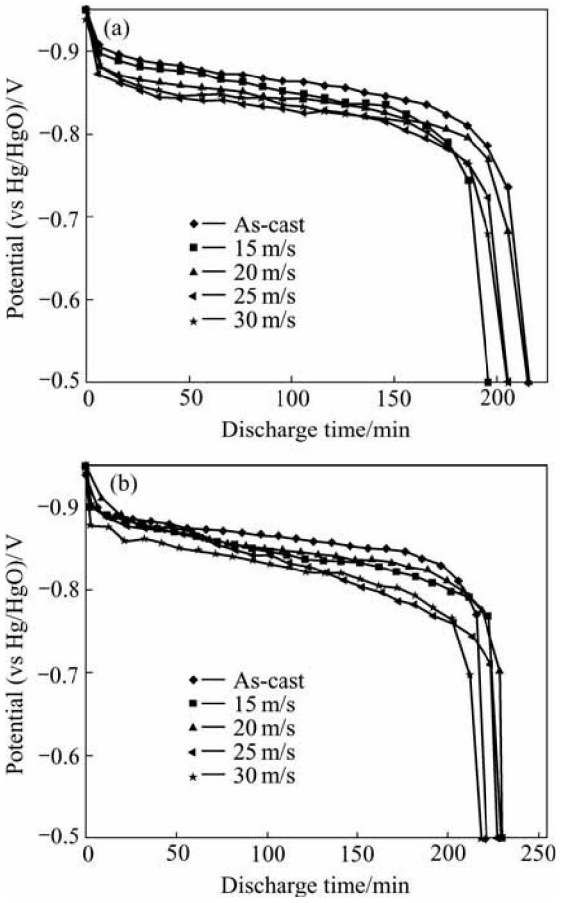

Fig.6 Discharge voltage curves of alloys quenched at different rates: (a) M_0; (b) M_1

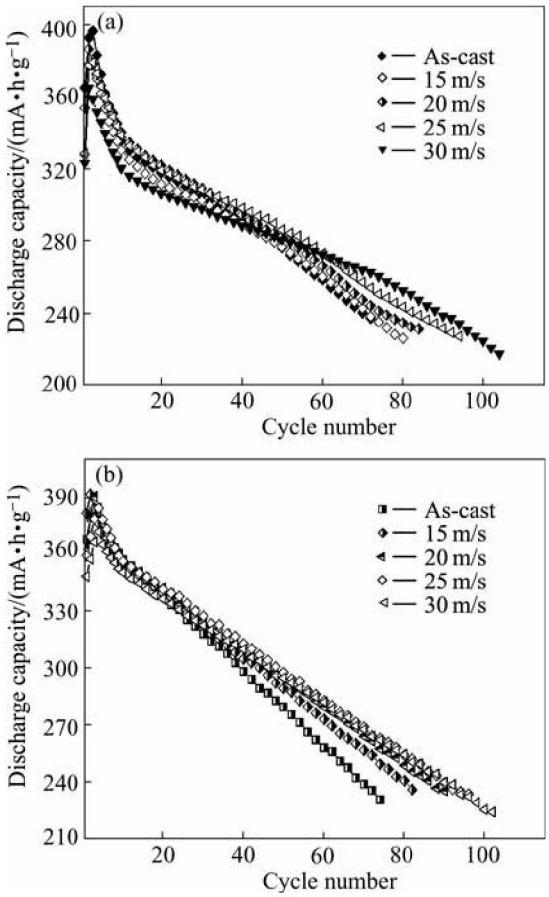

Fig.7 Relationship between cycle number and discharge capacity of alloys quenched at different rates: (a) M_0; (b) M_1

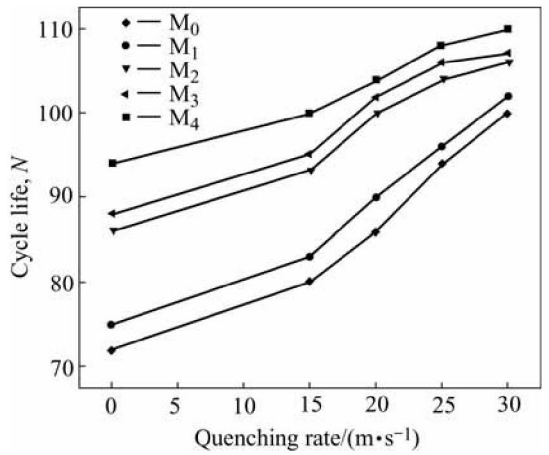

Fig.8 Quenching rate dependence on cycle life of alloys

It is confirmed in Ref.[13] that the fundamental reasons for the capacity decay of the electrode alloy are the pulverization and oxidation of the alloy during charge-discharge cycle. The lattice internal stress and cell volume expansion, which are inevitable when hydrogen atoms enter into the interstitials of the lattice, are the real driving force that leads to the pulverization of the alloy. The decisive factors of the anti pulverization capability of the electrode alloy are its strength and toughness. The main cause of rapid quenching enhancing the cycle lives of the alloys is ascribed to the grain refinement and the formation of an amorphous phase resulted from rapid quenching. The higher the quenching rate, the smaller the grain size of the alloy and the more the amount of amorphous phase, the higher the strength and toughness, the stronger the anti-pulverization capability and the longer the cycle life.

In order to correctly understand the mechanism of the efficacy loss of the electrode alloy, the particle morphologies of the as-cast and quenched alloys before and after electrochemical cycling as observed by SEM are shown in Fig.9. It can be seen from Fig.9 that the shapes of the as-cast and quenched alloy particles before electrochemical cycling are irregular and sharp-angled. After charge-discharge cycling, their morphologies change markedly, leading to a disappearance of the pointedness of the particle and to a decrease of the particle sizes. This indicated that the capacity decay of the alloy during electrochemical cycle is related to the pulverization of the electrode alloy. It is worthy to be noticed that the pulverization degree of the alloys after

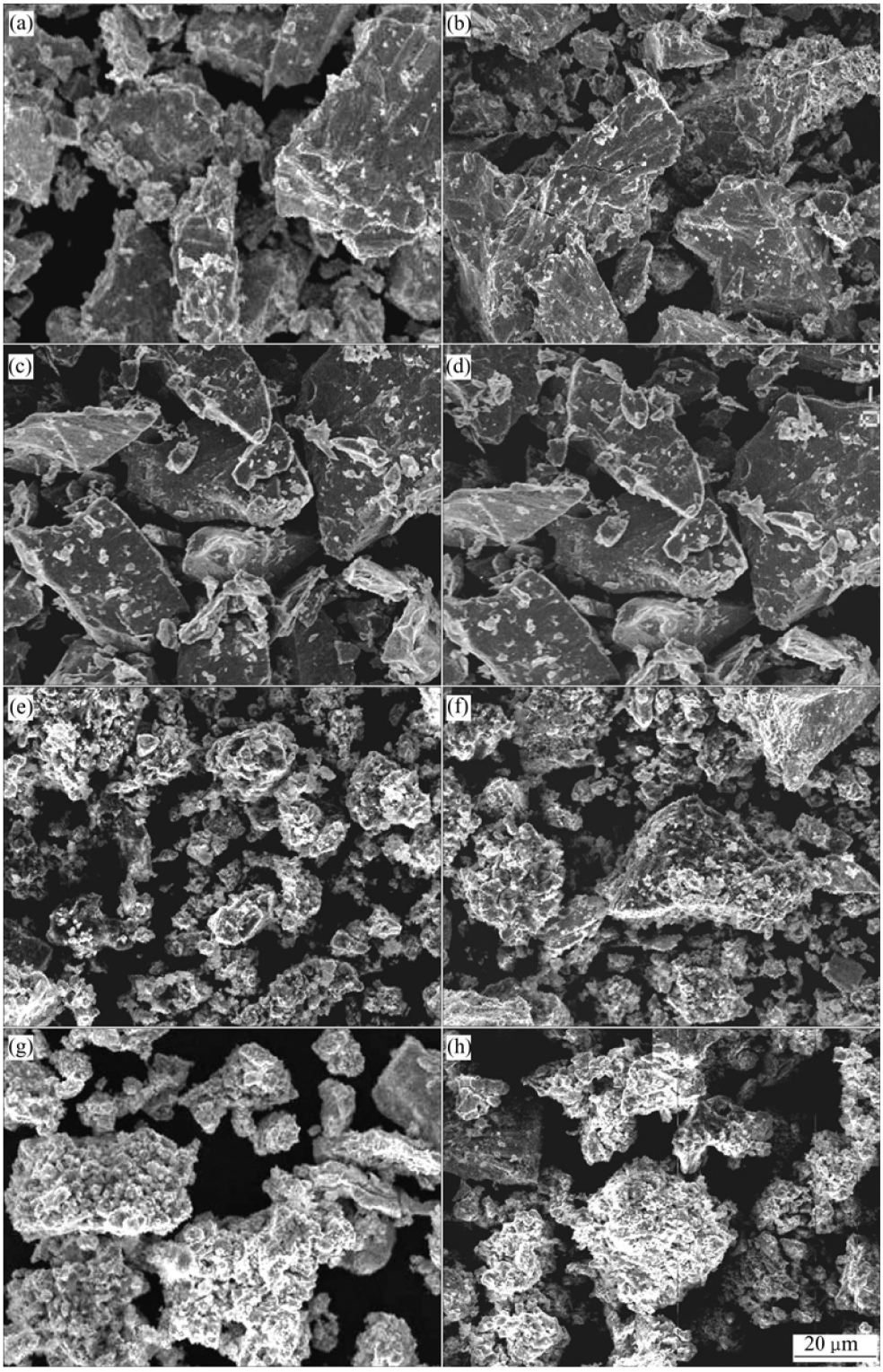

Fig.9 Granular morphologies of M_2 alloys before and after electrochemical cycle (SEM): (a), (b), (c) and (d) Before cycling of M_2 alloy with quenching rates of 0, 15, 20 and 30 m/s, respectively; (e), (f), (g) and (h) After cycling of M_2 alloy with quenching rate of 0, 15, 20 and 30 m/s, respectively

electrochemical cycling is obviously different. The pulverization of the alloy obviously decreases with the increase of the quenching rate. This indicated that rapid quenching could enhance the anti-pulverization capability of the alloy. Compared with the as-quenched AB_5-type hydrogen storage alloy, the pulverization degree of the La-Mg-Ni system alloy after electrochemical cycling is much smaller[14,15], and an oxidation and corrosion layer can be seen on the surface of the La-Mg-Ni system alloy after electrochemical

cycling. This indicated that the corrosion and oxidation is an important reason leading to the efficacy loss of the alloy. Therefore, it can be concluded that the improvement of the anti-corrosion and oxidation capabilities of the alloys produced by rapid quenching is very limited.

4 Conclusions

1) The as-cast and quenched $La_{0.7}Mg_{0.3}Ni_{2.55}Co_{0.45}$-$B_x$($x$=0, 0.05, 0.1, 0.15, 0.2) electrode alloys have a multi-phase structure, including (La, Mg)Ni_3 phase, $LaNi_5$ phase and a small amount of $LaNi_2$ phase. A trace of Ni_2B phase exists in the as-cast alloy containing boron and Ni_2B phase can increase the amount of $LaNi_2$ phase. Rapid quenching leads to an increase of the amount of $LaNi_2$ phase in M_0 alloy and a decrease in the B-containing alloys. This is ascribed to the approximate disappearance of Ni_2B phase resulted from rapid quenching.

2) The effects of rapid quenching on the capacities of the B-containing and B-free alloys are different. The capacity of the B-free alloy monotonously decreases with the increase of the quenching rate, whereas the capacities of the B-containing alloys have a maximum value with the change of the quenching rate. Rapid quenching lowers the discharge plateau voltage and obviously increases the slopes of the discharge voltage plateaus of the alloys when the quenching rate is more than 20 m/s.

3) The main reason of leading to the efficacy loss of the La-Mg-Ni based electrode alloy is the pulverization of the alloy during charge-discharge cycle, and the corrosion and oxidation of the alloy is also an important reason. Rapid quenching could significantly enhance the anti-pulverization capability of the alloy, but its action on the improvement of the anti-corrosion and oxidation capabilities of the alloys is very limited.

References

[1] UEHARA I, SAKAI T, ISHIKAWA H. The state of research and development for applications of metal hydrides in Japan [J]. J Alloys Comp, 1997, 253−254: 635−641.

[2] WANG Q D, CHEN C P, LEI Y Q. The recent research, development and industrial applications of metal hydrides in the People's Republic of China [J]. J Alloys Comp, 1997, 253−254: 629−634.

[3] HOUT J, AKIBA E, OGURA T, ISHIDO Y. Crystal structure, phase abundance and electrode performance of Laves phase compounds (Zr, A)$V_{0.5}Ni_{1.1}Mn_{0.2}Fe_{0.2}$ (A Ti, Nb or Hf) [J]. J Alloys Comp, 1995, 218: 101−109.

[4] TSUKAHARA M, KAMIYA T, TAKAHASHI K, KAWABATA A, SAKURAI S, SHI J, TAKESHITA H T, KURIYAMA N, SAKAI T. hydrogen storage and electrode properties of V-based solid solution type alloys prepared by a thermic process [J]. J Electrochem. Soc, 2000, 147: 2941−2944.

[5] SUN Da-lin, ENOKI H, GINGL F, AKIBA E. New approach for synthesizing Mg-based alloys [J]. J Alloys Comp, 1999, 285: 279−283.

[6] KADIR K, SAKAI T, UEHARA I. Synthesis and structure determination of a new series of hydrogen storage alloys; RMg_2Ni_9 (R=La, Ce, Pr, Nd, Sm and Gd) built from $MgNi_2$ Laves-type layers alternating with AB_5 layers [J]. J Alloys Comp, 1997, 257: 115−121.

[7] KOHNO T, YOSHIDA H, KAWASHIMA F, INABA T, SKAKI I, YAMAMOTO M, KANDA M. Hydrogen storage properties of new ternary system alloys: La_2MgNi_9, $La_5Mg_2Ni_{23}$, La_3MgNi_{14} [J]. J Alloys Comp, 2000, 311: L5−L7.

[8] PAN Hong-ge, LIU Yong-feng, GAO Ming-xia, ZHU Yun-feng, LEI Yong-quan, WANG Qi-dong. An investigation on the structural and electrochemical properties of $La_{0.7}Mg_{0.3}(Ni_{0.85}Co_{0.15})_x$($x$=3.15−3.80) hydrogen storage electrode alloys [J]. J Alloys Comp, 2003, 351: 228−234.

[9] ZHANG Yang-huan, CHEN Mei-yan, WANG Xin-lin, WANG Guo-qing, LIN Yu-fang, QI Yan. Effect of boron addition on the microstructures and electrochemical properties of $MmNi_{3.8}Co_{0.4}Mn_{0.6}Al_{0.2}$ electrode alloys prepared by casting and rapid quenching [J]. J Alloys Comp, 2004, 373: 291−297.

[10] LI Y, CHENG Y T. Amorphous La-Ni thin film electrodes[J]. J Alloys Comp, 1995, 223: 6−12.

[11] WU Mao-sung, WU Hong-rong, WANG Yung-yun, WAN Chi-chao. Surface treatment for hydrogen storage alloy of nickel/metal hydride battery [J]. J Alloys Comp, 2000, 302: 248−257.

[12] LI Ping, WANG Xin-lin, ZHANG Yang-huan, LI Rong, WU Jian-min, QU Xuan-hui. Research on electrochemical characteristics and microstructure of $Mm(NiMn\text{-}Al)_{4.9}Co_{0.2}$ rapidly quenched alloy [J]. J Alloys Comp, 2003, 353: 278−282.

[13] CHARTOUNI D, MELI F, ZÜTTEL A, GROSS K, SCHLAPBACH L. The influence of cobalt on the electrochemical cycling stability of $LaNi_5$-based hydride forming alloys [J]. J Alloys Comp, 1996, 241: 160−166.

[14] ZHANG Yang-huan, WANG Guo-qing, DONG Xiao-ping, GUO Shi-hai, WANG Xin-lin. Effects of rapid quenching on the electrochemical performances and microstructures of the $Mm(NiMnSiAl)_{4.3}Co_{0.6-x}Fe_x$ (x=0−0.6) electrode alloys [J]. J Power Sources, 2004, 137: 309−316.

[15] ZHANG Yang-huan, DONG Xiao-ping, WANG Guo-qing, et al. Cycling stability of La-Mg-Ni system ($PuNi_3$-type) hydrogen storage alloy prepared by casting and rapid quenching [J]. The Chinese Journal of Nonferrous Metals, 2005, 15(5): 705−710.(in Chinese)

(Edited by LONG Huai-zhong)